LA-UR- 96-3677

Title: RANGE-GATED IMAGING FOR NEAR-FIELD TARGET IDENTIFICATION

CONF-9610181--3

Author(s): George J. Yates, Robert A. Gallegos, and Thomas E. McDonald
Los Alamos National Laboratory, P-23

Fred J. Zutavern, Wesley D. Helgeson, and Guillermo M. Loubriel, Sandia National Laboratories

Submitted to: SPIE 22nd International Congress on High-Speed Photography and Photonics

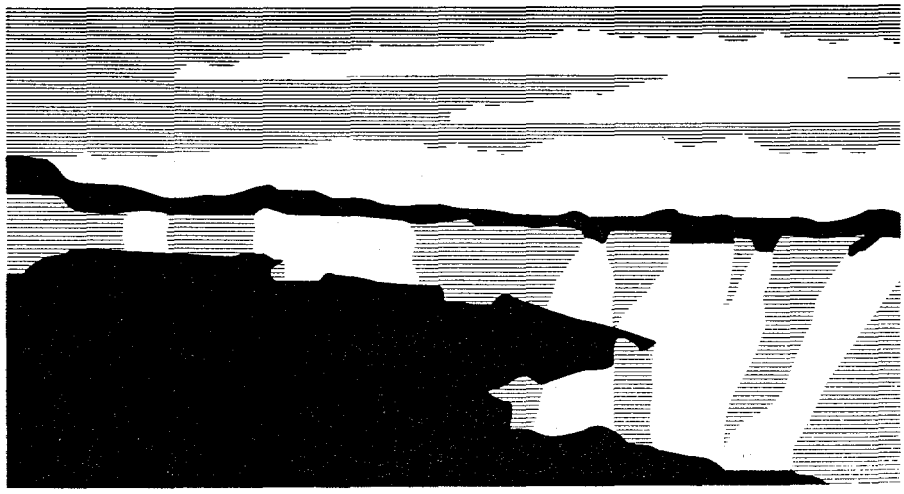

Los Alamos
NATIONAL LABORATORY

Form No. 836 R5
ST 2629 10/91

DISCLAIMER

Range-gated imaging for near-field target identification

George J. Yates, Robert A. Gallegos, and Thomas E. McDonald

Los Alamos National Laboratory, P-23, MS H803 Los Alamos, NM 87545

Fred J. Zutavern, Wesley D. Helgeson, and Guillermo M. Loubriel

Sandia National Laboratories, P.O. Box 5800, Albuquerque, NM 87185-1153

ABSTRACT

The combination of two complementary technologies developed independently at Los Alamos National Laboratory (LANL) and Sandia National Laboratory (SNL) has demonstrated feasibility of target detection and image capture in a highly light-scattering medium. The technique uses a compact SNL developed Photoconductive Semiconductor Switch/Laser Diode Array (PCSS/LDA) for short-range (distances of 8 to 10 m) large Field-Of-View (FOV) target illumination. Generation of a time-correlated echo signal is accomplished using a photodiode. The return image signal is recorded with a high-speed shuttered Micro-Channel-Plate Image Intensifier (MCPII), designed by LANL and manufactured by Philips Photonics. The MCPII is gated using a high-frequency impedance-matching microstrip design to produce 150 to 200 ps duration optical exposures. The ultra fast shuttering produces depth resolution of a few inches along the optic axis between the MCPII and the target, producing enhanced target images effectively deconvolved from noise components from the scattering medium in the FOV. The images from the MCPII are recorded with an RS-170 Charge-Coupled-Device camera and a Big Sky, Beam Code, PC-based digitizer frame grabber and analysis package. Laser pulse data were obtained by the system but jitter problems and spectral mismatches between diode spectral emission wavelength and MCPII photocathode spectral sensitivity prevented the capture of fast gating imaging with this demonstration system. Continued development of the system is underway.

Key Words: target detection, image capture, 150 to 200 ps optical exposures, PCSS/LDA, MCPII

2. INTRODUCTION

The combination of two complimentary technologies developed independently at Los Alamos National Laboratory (LANL) and at Sandia National Laboratories (SNL) have been tested for use in a range gated application for target detection and imaging over short distances in a highly light-scattering medium. An application of interest is imaging over ranges of approximately 25 feet in highly turbid water, such as might be encountered near the surf zone of the ocean. The approach was to use a SNL developed compact Photoconductive Semiconductor Switch (PCSS) and Laser Diode Array (LDA), which has a relatively wide divergence angle of approximately 15 degrees, and a LANL developed intensified, gated imager set up in an active range gating configuration.

The idea of active range gating is well known and is illustrated in Fig. 1. [1,2] Conceptually the approach can be used to image targets hidden by light scattering media such as in hazy atmospheric conditions, clouds and fog, and turbid water. In an active range gating system the target is illuminated by a pulsed laser beam having a short pulse width of a few nanoseconds or sub-nanoseconds. The return signal is detected by a gated image intensifier, which is timed to intensify light only during a narrow time interval at the time the light from the vicinity of the target region has returned. Background and foreground objects are not illuminated by the narrow pulse and backscattered light from the light scattering media arriving during intensifier off time is eliminated. Thus, the gated detection system significantly reduces the noise or unwanted light scattered from the intervening media into the captured image and effectively increases the signal-to-noise ratio. By gating

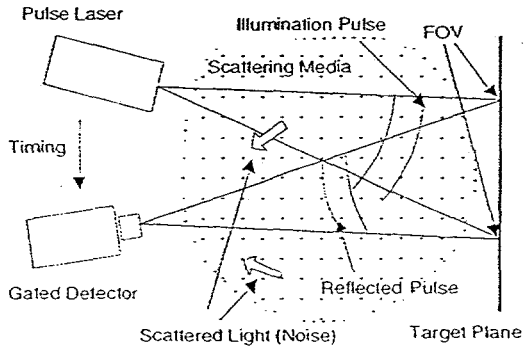

Fig. 1. The laser source illuminates the target with a short pulse and provides a timing signal to the gated detector. The gated detector is set to accept light from the vicinity of the target plane and reject most of the light scattered by the intervening media.

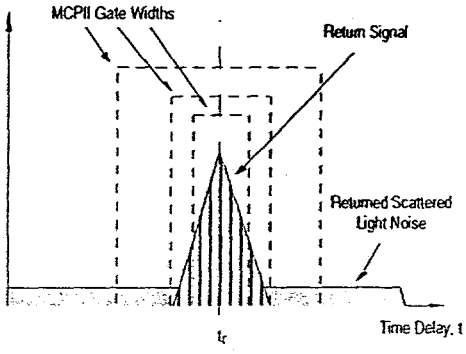

Fig. 2. The light pulse from the target arrives at the detector after a delay in time, t_r, due to the flight distance from the pulsed source. The detector gate time, t_{g2}, is set to coincide with the returning pulse. At time t_{g1} the gate is set too early and at t_{g3} the gate is delay too late.

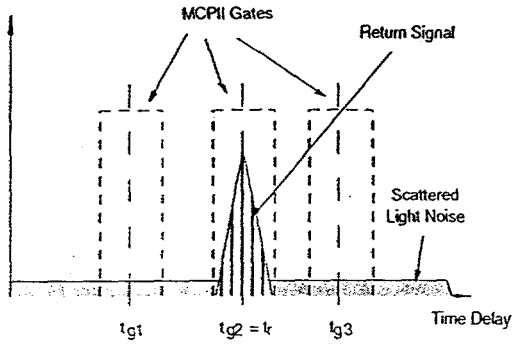

Fig. 3. Gate widths that are too wide accept more scattered light noise than necessary and widths that are too narrow reject part of the signal pulse and, thus, reduce the signal strength with little increase in S/N. The optimum gate width is approximately the width of the illuminating pulse.

the intensifier on for, say, 5 ns to detect a target 1000 ns away in total light path (approximately 500 ft) 99.5% of the unwanted scattered light is eliminated from the image. If the intensifier gate is 500 ps, 99.95% of the scattered light is eliminated. The tradeoff is that at the short gate widths, the signal is also reduced. If, however, the pulse width of the illuminating beam is the same width as the intensifier gate, say 500 ps, then the scattered light noise is eliminated without a concomitant reduction in integrated signal at the detector. Thus, the highest signal strength and overall signal to noise ratio is achieved when the detector gate width matches the illuminating pulse width. Figures 2 and 3 illustrate the concept.

3. FAST-GATED IMAGE INTENSIFIER

Fast optical shuttering using proximity focused microchannel plate (MCP) image intensifiers (MCPII) is accomplished by suppression of photo-electrons from the photocathode. This is accomplished by reverse-biasing the photocathode- to-MCP interface, as illustrated in Fig. 4. For nanosecond and subnanosecond shutters, this requires special processing of the intensifier photocathode to increase it's conductivity (reduce it's resistivity) and redesign of the intensifier package to provide transmission line geometry for gate pulse injection and propagation of the electrical pulse across the gated surfaces within the MCPII.

The intensifier design is essentially a modification of Generation-2 18-mm-diameter night vision goggles originally designed for use by the US military. The current design is an evolution of several iterations. Modeling of the original MCPII design as a radial transmission line comprised of distributed R and C elements [3] defined speed related parameters required for nanosecond shuttering. The principal limitation was the RC time constant associated with the MCPII's photocathode impedance (dominated by the effective sheet resistance of typical S-20 cathodes, approx. 10^3 to 10^6 Ω/sq) and the photocathode-to-MCP "gap" capacitance. Various electrically conductive optically transmissive coatings were evaluated and nickel was selected for photocathode underlayer which provided 50 to 150 ohms/square sheet resistance with typical 50% optical transmission. The important "gap" capacitance (approx. 27 pfd) was shunted by peripheral capacitances associated with the tube structure, compounding the difficulty of correct modeling. Various designs were generated which resulted in varying degrees of success in improving shutter speeds. Most designs were characterized by "irising" during the shutter sequence. [4,5]

Our most recent designs [6,7] are based on stripline MCPIIs which are essentially "lossy" transmission lines with low inductance gate pulse insertion point at one side of the MCPII and exit point geometrically 180 degrees at opposite end of the MCPII as illustrated in Fig 5. These MCPIIs have been modeled as transverse transmission lines with "gap" impedance of approximately 4 to 5 ohms when driven with nanosecond and subnanosecond gate pulses, i.e., their effective impedance at GHz frequencies. The impedance corresponding to the adjacent peripheral internal tube structures varies widely, even with our earlier Stripline designs. Recent first-approximation calculations of impedance variance across the MCPII are highlighted in Fig. 6 and tabulated in Table 1 for the existing earlier first-generation

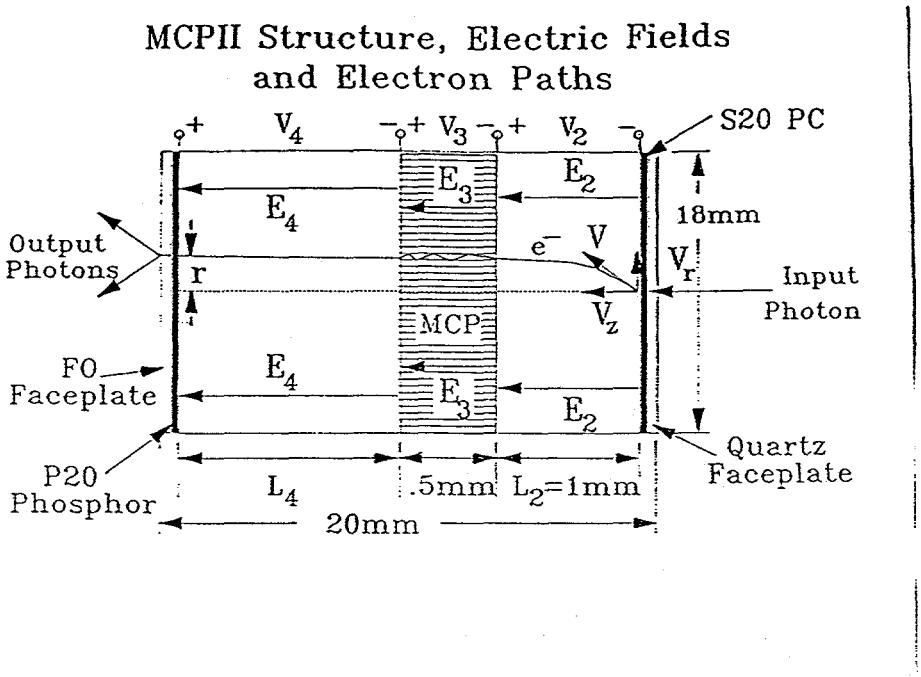

Fig. 4. Functional diagram of MCPII optical shutter.

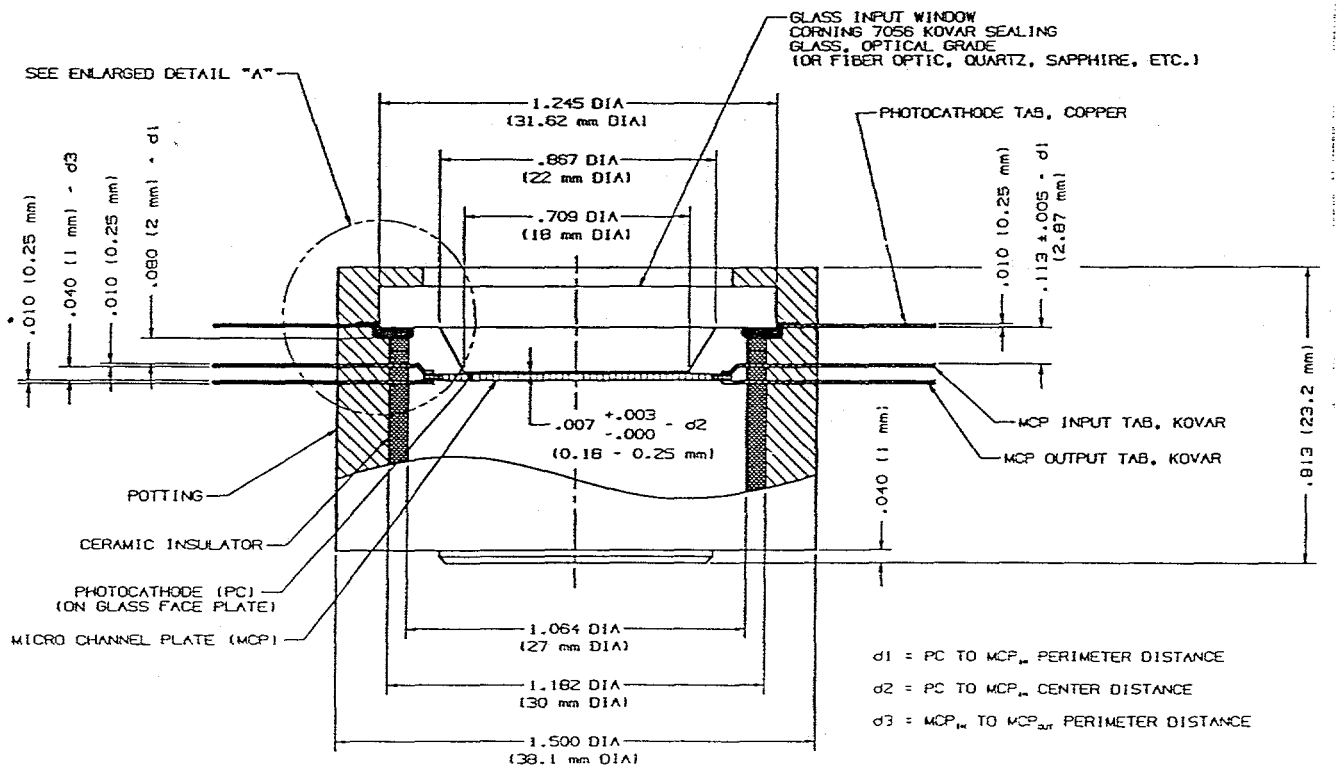

Fig. 5. Mechanical schematic of Stripline MCPII showing low inductance planar tabs on photocathode and MCP electrodes for mating with Microstrip gate pulse drivers.

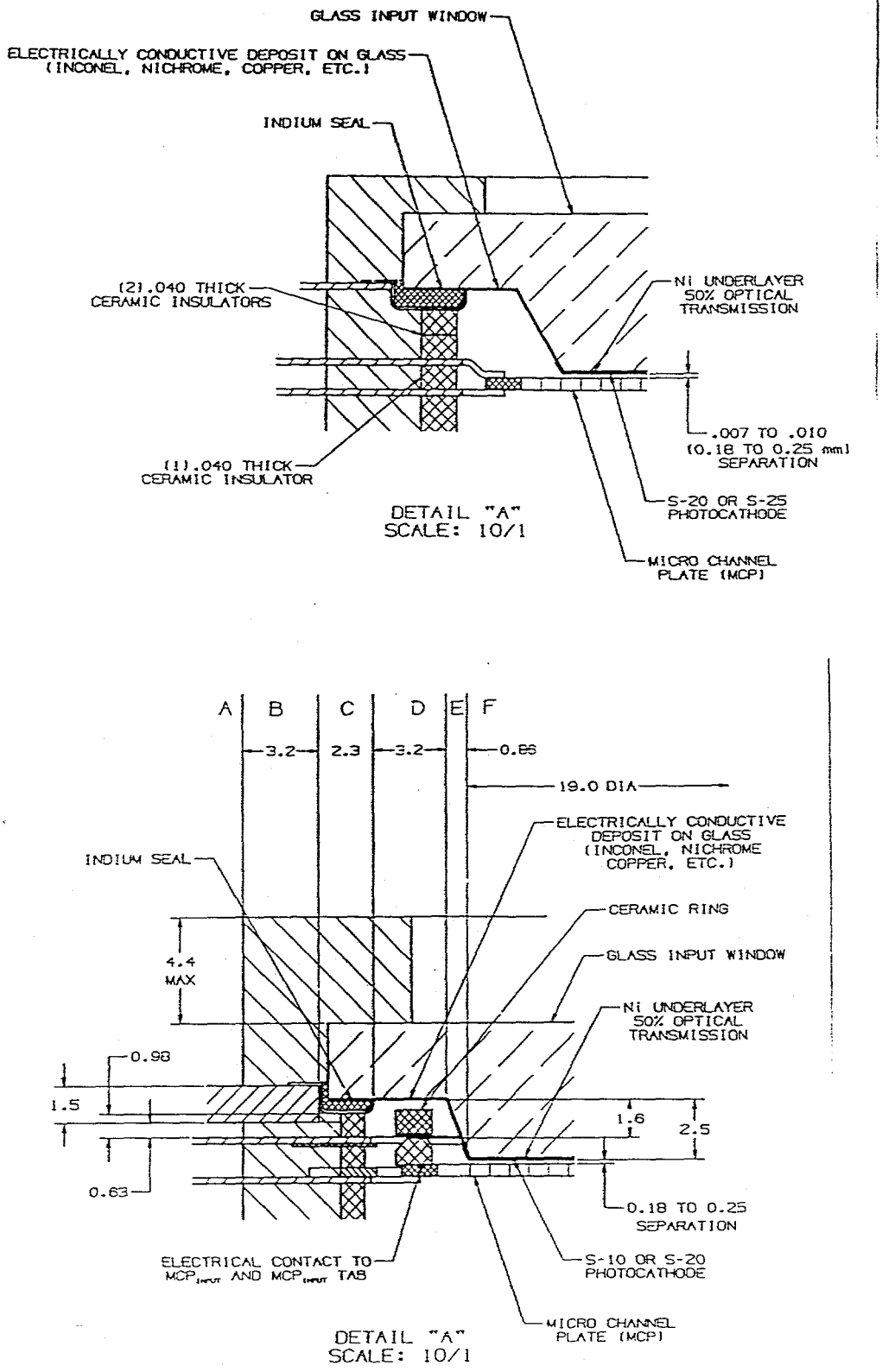

Fig. 6. Schematics of our first-generation (top) and second-generation (bottom) Stripline MCPII designs highlighting differences between the two that actually produce different impedances for the same regions, i.e., A through F.

Table 1. Calculated impedance values (based upon indicated dimensions and dielectric constant) for various sections of first-generation (parenthesized entries) and second-generation Stripline MCPII designs. For region F, F1 is for circular photocathode and F2 is for rectangular photocathode.

Region	Dielectric Constant	L (mm)	W (mm)	H (mm)	Z (ohms)
A	(1) 9	(5.0) 5.0	(6.4) 9.5	(2.9) 0.63	(85) 7.3
B	(3) 3	(3.3) 3.3	(7.0) 10	(2.9) 0.63	(51) 11.9
C	(9) 9	(2.3) 2.0	(10.0) 10	(2.1) 0.98	(19) 10.3
D	(1) 9	(2.5) 2.0	(12.0) 12.3	(2.9) 1.55	(57) 12.7
E	(1) 1	(2.1) 0.86	(14.0) 14.6	(1.4) 0.86	(29) 18.7
F1	(1) 1	(16) 16.8	(16.0) 16.8	(0.2) 0.20	(4.5) 4.3
F2	(1) 1	(16) 16.8	(16.0) 9.0	(0.2) 0.20	(4.5) 7.3

stripline design. This has helped further identify areas for redesign to reduce the impedance variance. A second generation stripline design incorporating changes shown in Fig. 6b is currently in fabrication phase. The principal changes are (1) inclusion of internal ceramic ring to occupy the internal space near the perimeter of the MCPII corresponding to the area adjacent to the input glass or fiber optic faceplate taper (region B, Fig. 6b). This provides a dielectric constant of 9 in place of the dielectric constant of 1 for vacuum, and modifies the impedance in this region of the tube as noted in Table 1; (2) reduction of the tube volume associated with the taper by thinner faceplate thickness and steeper slope for the taper; and (3) a narrower spacing between the external photocathode and MCP tabs to correspond to the dielectric and printed circuit board thickness of the tapered microstrip impedance transformers (see Fig. 7) used to launch the electrical gate pulse to shutter the MCPII. Stripline MCPIIs without mod (3) require the use of an extremely high dielectric material in this region (region A, Fig. 6b), such as Barium (or Strontium) Titanite, which have a dielectric constant of about 100 at GHz frequencies. The calculated impedances across the various regions of the new second generation stripline MCPII design are identified in Fig. 6b and Table 1. Refined modeling using ANSOFT, Corp., Maxwell 3D Field Simulator, is in progress. Impedance calculations using Maxwell Equations will be forthcoming to refine our first-approximation estimates cited in Table 1.

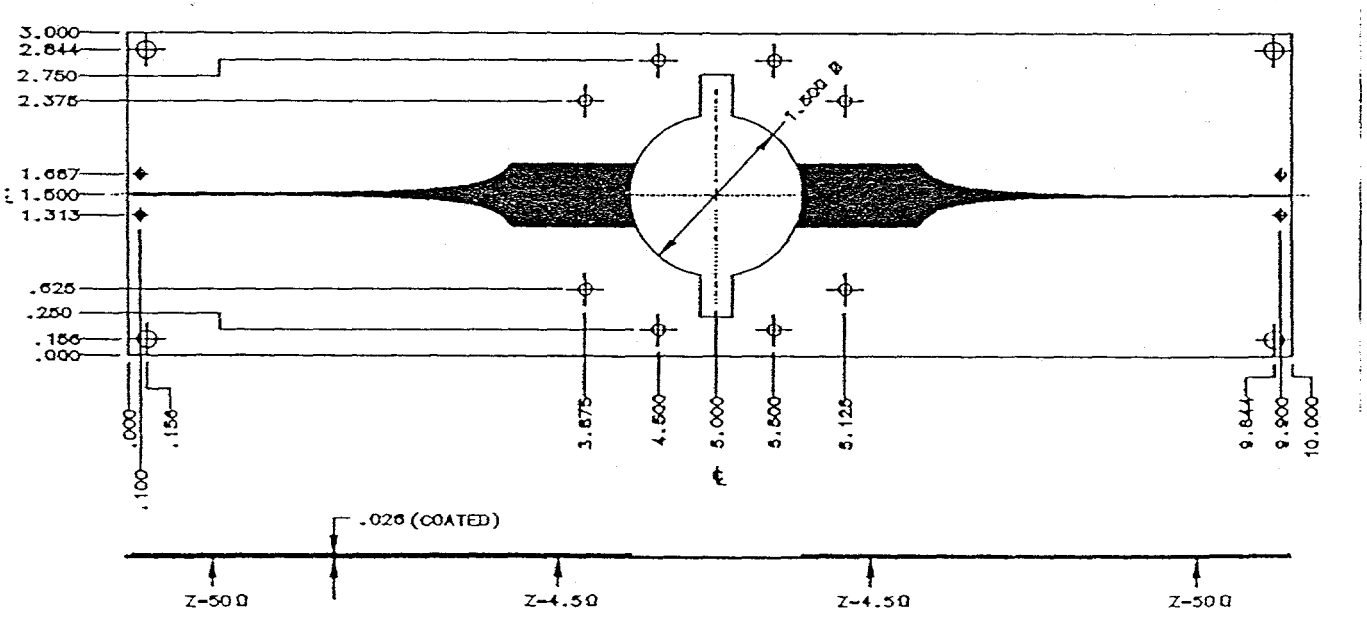

Fig. 7. Layout of the 50-ohm to 4.5-ohm impedance transformer Microstrip gate pulse insertion driver for the Stripline MCPII.

4. TDR AND NETWORK ANALYZER MEASUREMENTS ON MICROSTRIP AND MCPII

The microstrip impedance transformers were measured with and without the MCPII in the circuit using an Hewlett Packard 5412A sampling oscilloscope network analyzer to characterize the individual and combined responses to short duration gate pulses. The pulse attenuation is expected to go as the square root of the ratio of the higher impedance (50 ohms) to the lower impedance (4.5 ohms), which is 3.33X. We believe this to be the case for pulse widths that are within the frequency bandwidth of the transformer. For the bandwidth-limited case, we expect the pulse energies at the two impedances to reflect the above attenuation factor. Only the measurements for the combined microstrip/MCPII are discussed. For input pulse, at the 50-ohm end, of approximately 1000V and 300 pS FWHM we observed about 350V and 250 pS FWHM for the 4.5-ohm section of the microstrip. This is close to the expected amplitude of 300V. The ratio of energies is 3.43X, which is close to the expected value. For a much narrower input pulse width of about 25 pS FWHM and 2.8V, the 4.5-ohm section measured 0.15V and 140 pS FWHM. For this case, the amplitude attenuation and increased pulse width are expected because the input stimulus exceeded the design bandwidth of the microstrip transformer. The energy ratios are as expected, i.e., 3.33X. The data for FWHM pulses of 220 pS, 725 pS, and 8.9 ns are shown in Fig. 8.

We originally attempted TDR measurements, using a Tektronix 11801B digital sampling system as a method for observing the impedance variance within the Stripline MCPII internal structure, which is inaccessible for external probing. However, analysis of the TDR reflected waveforms from complex geometries such as the MCPII involving multiple impedance mismatches are difficult to interpret directly. This is because at each mismatch, a new amplitude and polarity of reflection from the preceding waveform must be used since the initial step waveform from the TDR only correctly characterizes the first mismatch. For this reason, we feel our TDR data are reasonably correct only for the first and second major impedance variances encountered in the circuit or component under test.

We performed TDR measurements on the microstrip transformer first, with no MCPII attached to the 4.5-ohm section, but rather left it either open or terminated with a wide piece of conductive copper tape shorting the section to the ground plane of the microstrip. The measurement indicated a varying impedance from 50 ohms to 4.5 ohms as expected and transition towards either open circuit (reflection coefficient of +1) or short circuit (reflection coefficient of −1) as indicated in the top and bottom waveforms of Fig. 9b. The propagation constant was varied until the electrically measured length indicated by the TDR (Fig. 9a) agreed with the actual physical dimensions (2.9 in) of the microstrip. This was found to be 0.38 (corresponding to 38% of the speed of light in vacuum) for the microstrip transformer as compared to 0.54 for a single impedance 50-ohm microstrip, which was fabricated on similar printed circuit material. This difference in propagation velocity is not expected and is being studied.

Next we measured one of our first-generation Stripline MCPII separately and observed its impedance to be on the order of 15 ohms. This measurement was not in good agreement with our calculations or models. The particular intensifier had been damaged in testing and was no longer operational, which may have contributed to the measurement. We repeated the measurement on our second-generation Stripline MCPII which indicated about 9 ohm impedance as shown in Fig. 10b, which is much closer to expected value associated with perimeter impedance. As indicated above, the TDR data reflect primarily the first impedance seen as the step function propagates into the MCPII, so the impedance of the photocathode-to-MCP, which is well into the MCPII structure, cannot be measured directly from the TDR waveform without appropriate normalization. The transition time across the MCPII is shown in Fig. 10a for propagation constant of 0.44, which gave measured electrical length equal to the physical length of 1.75 in. between input and output photocathode tabs.

5. PREVIOUS RESULTS

The concept of imaging in highly scattering media through the use of range gating has been demonstrated in our earlier experiment. [2] In this demonstration a 20-ps FWHM laser pulse, 559 nm wavelength, was used to illuminate a target (Air Force resolution chart) that was submerged in an 18 inch tank filled with a colloidal suspension of tincture green soap in water. The detector was our first generation Stripline MCPII coupled to an RS-170 video camera with a Big Sky Technologies, Inc. BEAMCODE frame grabber used to capture the data. An impedance matching microstrip line was used to transition the pulse from an 50 ohm coaxial cable to the 4.5 ohm input of the MCPII. The MCPII was shuttered with either a 8 ns, 750 ps, or 250 ps, FWHM gating pulse. Although the gate width was well away from the more optimum gate width of approximately 50 ps, the results clearly demonstrated the capability of short gate widths to image through scattering media. The test pattern target was beginning to be distinguishable with the 750 ps gate width and significant improvement was seen in the image with the 250 ps gate width. Fig. 11 shows the results of these tests.

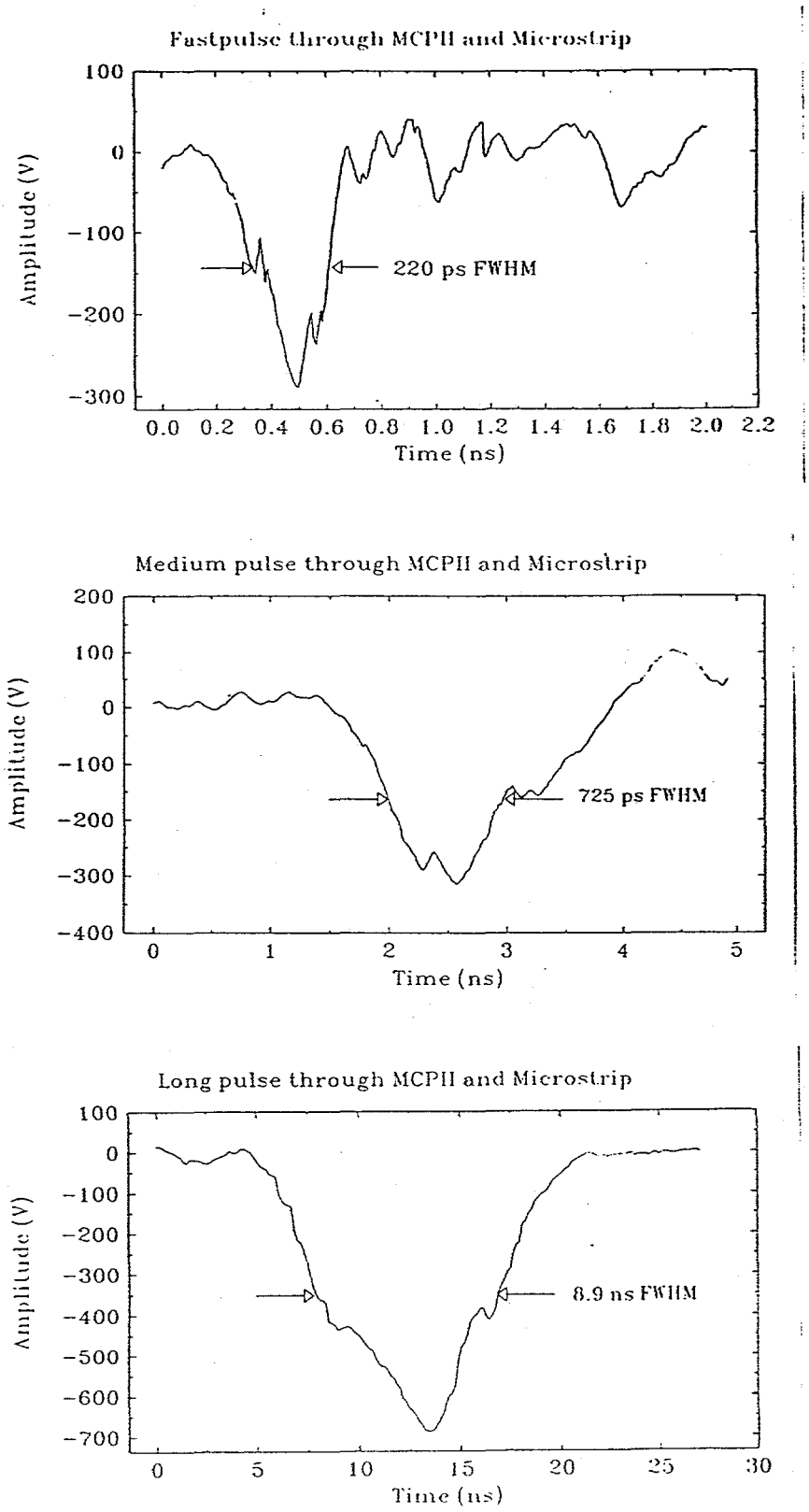

Fig. 8. Combined Microstrip/Stripline MCPII response, for driving pulse amplitude of −1000V, obtained using the Hewlett Packard Sampling Oscilloscope to measure the input waveforms and the waveforms after they have traversed both microstrip and intensifier. The attenuation for the 200 pS (top) and 725 pS (center or middle) FWHM pulses is about 3.33X, as expected. The longer 8.9 ns FWHM pulse (bottom) is attenuated only 1.4X because the impedance is frequency dependent.

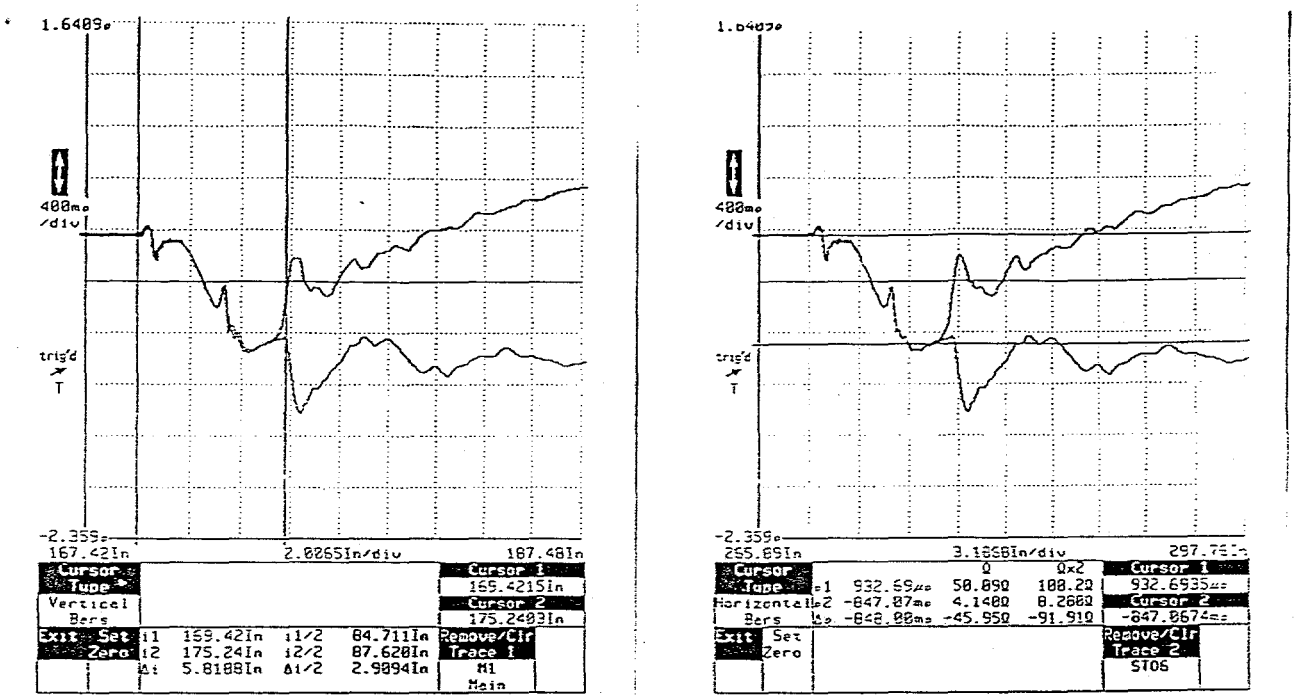

Fig. 9. The TDR data for the Microstrip alone taken with the Tektronix Sampling Oscilloscope. The transit time across the entire input half of the strip (up to the place where the MCPII is inserted) is shown in (a) and the impedance across the taper is in (b).

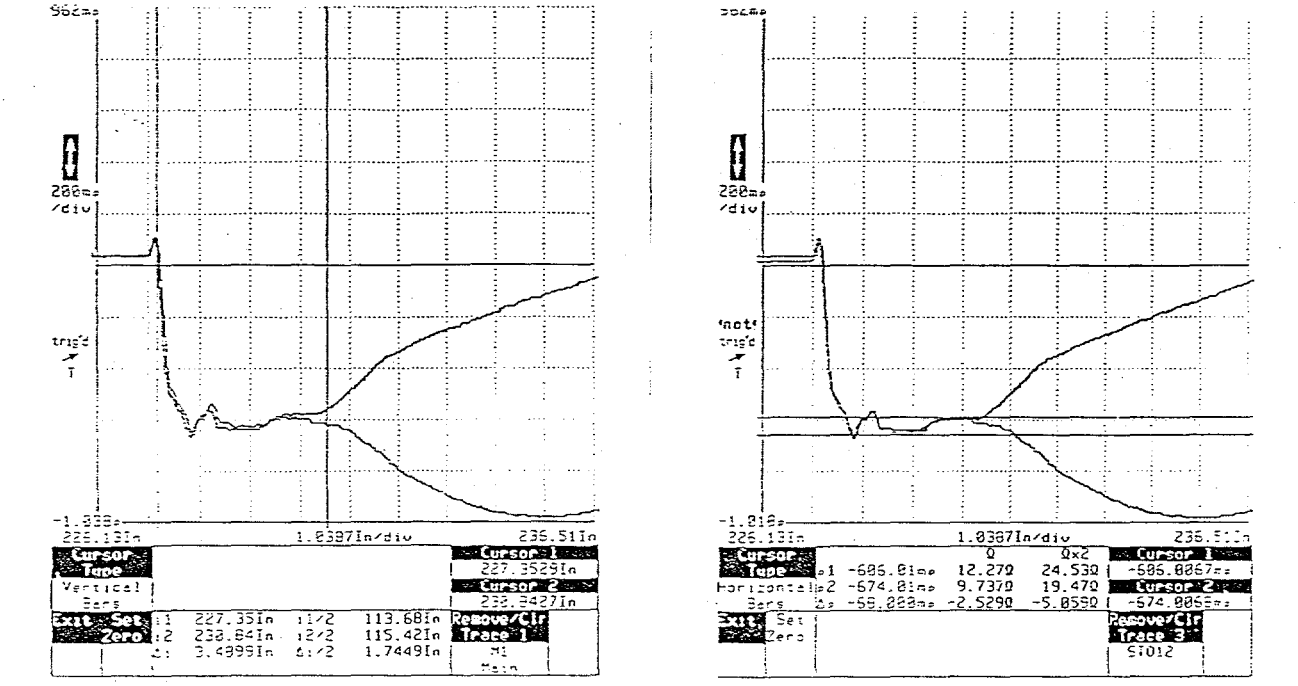

Fig. 10. The TDR data for the second-generation Stripline MCPII alone are shown as transition time defining the electrical length from input to output tabs of the photocathode in (a) and showing impedance across the MCPII in (b).

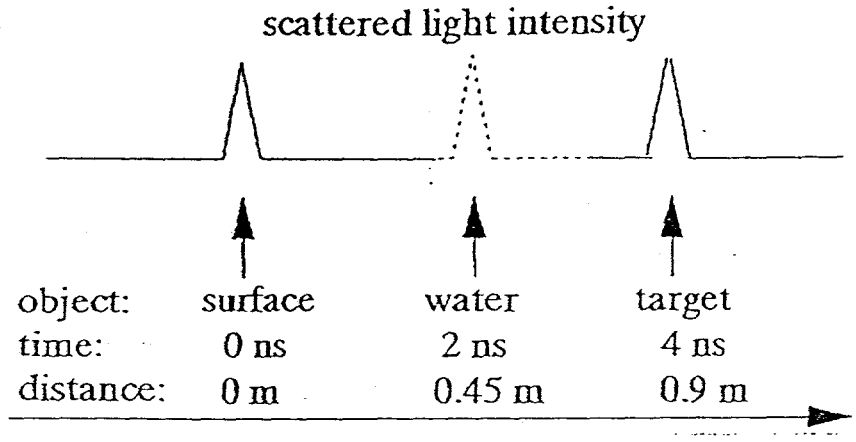

(a) Timing diagrams for image sequences in (b) and (c). The time-of-arrival (TOA) of the laser pulse at the three media is indicated with variable TOA for the water.

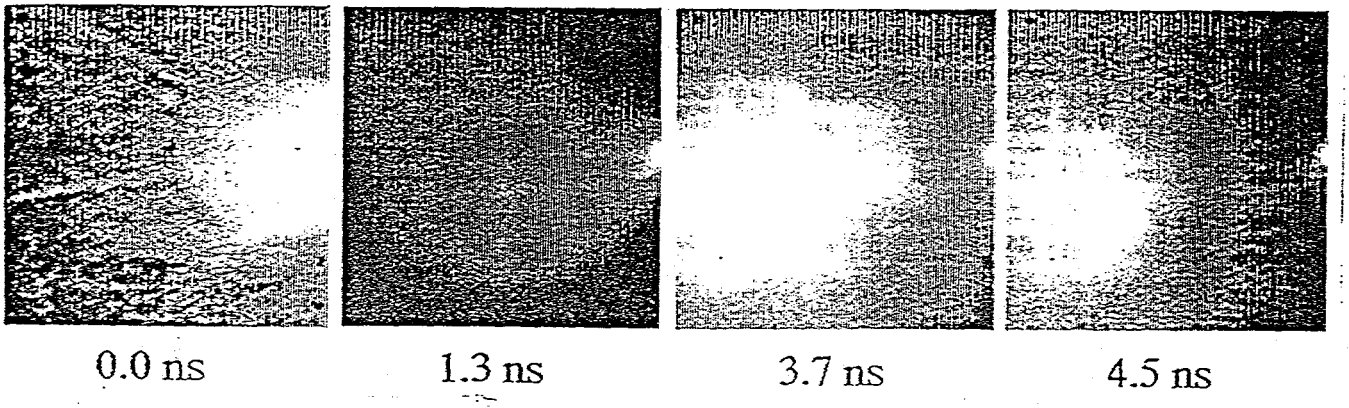

(b) Images from 750 pS first-generation Stripline MCPII shutter.

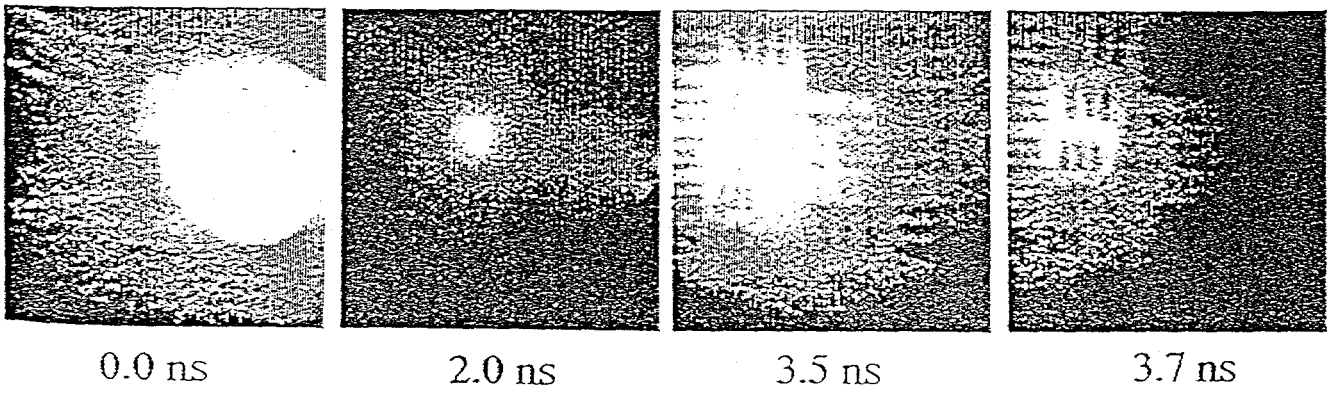

(c) Images from 250 pS first-generation Stripline MCPII shutter.

Fig. 11. Image enhancement data from our earlier range-gated experiment (a), illustrating increasing resolution from progressively shorter shutters, in (b) and (c). The sequence of images are (left) the laser reflection off the glass wall of the fish tank, (second) laser beam scattering in the water, (third) and (right) mix of laser beam illuminating target and surrounding water in the tank..

6. EXPERIMENTAL SETUP

With the encouraging results previously obtained, Los Alamos and Sandia collaborated on a system demonstration using the SNL PCSS/LDA to provide a pulsed illumination source and the Los Alamos fast-gated MCPII coupled to a CCD camera for image capture. The LDA has a relatively wide divergence angle and is, thus, best suited for imaging over short ranges requiring larger FOV than that provided by a coherent laser beam. The PCSS/LDA illuminator has the advantage of small size, light weight, and relatively low power requirements. The pulse width of the PCSS/LDA is a few nanoseconds and operates at a wavelength in the neighborhood of 904 nm. A description of the illuminator is given in a companion paper. [8] The MCPII is described in sections 2 and 3 above. A block diagram of the test system is shown in Fig. 12.

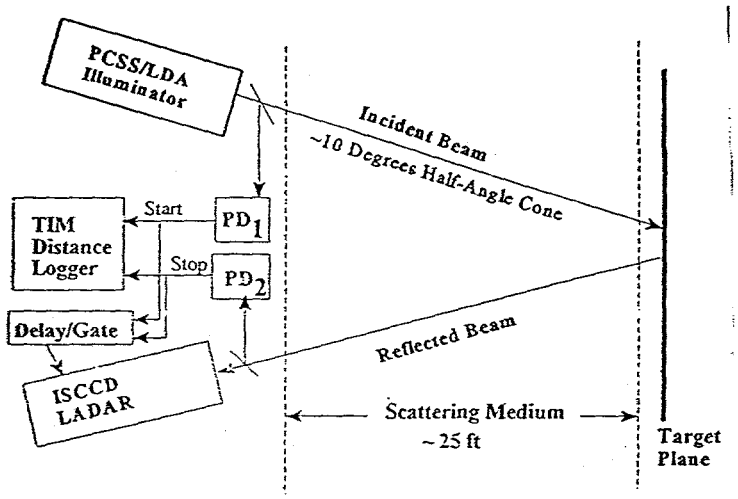

Fig. 12. The conceptual diagram for the SNL/LANL range-gated LIDAR/LADAR experiment to obtain both images and their distance/location.

The experiment encountered two problems immediately. First, the LDA's narrow-band emission was peaked at 904–910 nm, which is outside the spectral sensitivity curve for the MCPII's S-20 photocathode. This spectral mismatch made their combined responsitivity too poor for continuing with the imaging experiment. We decided to rectify the problem by (1) selecting a different LDA with emission wavelength within the S-20 response and also more suitable for transmission in water, such as 532 nm; and (2) in the short term, selecting an Extended Red photocathode such as InGaAs, which has higher QE at the 904–910 nm than does the S-20. At this writing, neither (1) nor (2) has been implemented yet, although both are in progress, (1) by SNL and (2) by LANL. The second major problem was that the PCSS/LDA had excessive time jitter, on the order of tens of nanoseconds, which made time phasing of the light pulse with the MCPII shutter opening difficult. Although the LDA pulse duration of a few nanoseconds would provide effective range resolution, the excessive time jitter would produce image data from several different locations and would arrive out of sync with the MCPII shutter opening.

The trigger pulse passes through one delay timer to the MCPII gate and a second delay timer to the LDA pulser. These delay times can be adjusted so the returning laser pulse falls within the gate of the MCPII. The delay times take into account the delays in the MCPII gate generator circuits and in the PCSS/LDA illuminator circuits. In order for the return pulse of the LDA to fall within the gate of the MCPII, the jitter of the gate generator circuits and the laser pulse generator circuits must be within a few tens of a percent of the gate width. Since it is desired to operate with a gate width of a nanosecond or less, the jitter of these paths must be of the order of a few tens to hundreds of picoseconds.

The jitter of the electronics circuitry has be found to be well within the system requirements. However, the jitter of the PCSS was found to be few tens of nanoseconds and increased with time of operation. Such jitter in laser pulse generation is typical and is usually solved by using a fast photodiode detector to sense the laser pulse as it leaves the laser and use the output of the photodiode as a trigger signal for the MCPII gate. The photodiode trigger signal is conditioned and sent through a delay timer to synchronize the MCPII gate to the returning laser pulse. The approach works well when the round trip time of the laser illumination pulse is at least as long as the intrinsic delay in the trigger path and gate circuitry. In the short range application, however, the laser pulse round trip time is a few to a few tens of nanoseconds and much of this range time is shorter than the delay through the gate circuitry.

To solve this problem, either the jitter in the PCSS/LDA must be reduced or the delay time between the gate trigger input and gate pulse generation must be reduced. At the present time we are examining reducing the intrinsic delay of the gate trigger circuitry. If this can be satisfactorily accomplished a system can be developed as shown in the block diagram of Fig. 12. The time between photodiodes one and two would determine the distance to the target and would also be used to trigger and control the timing of the MCPII gate.

7. RESULTS

Range-gated images were not obtained for the reasons stated above. However, we did obtain images from the PCSS/LDA, using the MCPII/CCD recorded with Beam Code RS 170 frame grabber. Images of the five bars of laser diodes comprising the LDA were acquired and averaged to improve image statistics. At room temperature, the laser diode emission was barely picked up by the MCPII, but we found that by cooling the LDA, its emission wavelength shifted about 15 nm toward (shorter) the top edge of the S-20 response, improving the MCPII signal by approximately 20X. The "cooled" data are shown in Fig. 13, which is an average of ten frames as noted in Table 2. These light signals, file "warm 9" of Table 2, are from the five bars, with the digitizer cursors through one of the five bars to give intensity profiles. The "warm" or "non-cooled" data entries in Table 2 show the improvements from the cooling of the LDA, which are indicative of signal-to-noise attainable with better spectral matching of PCSS/LDA to MCPII for future experiments.

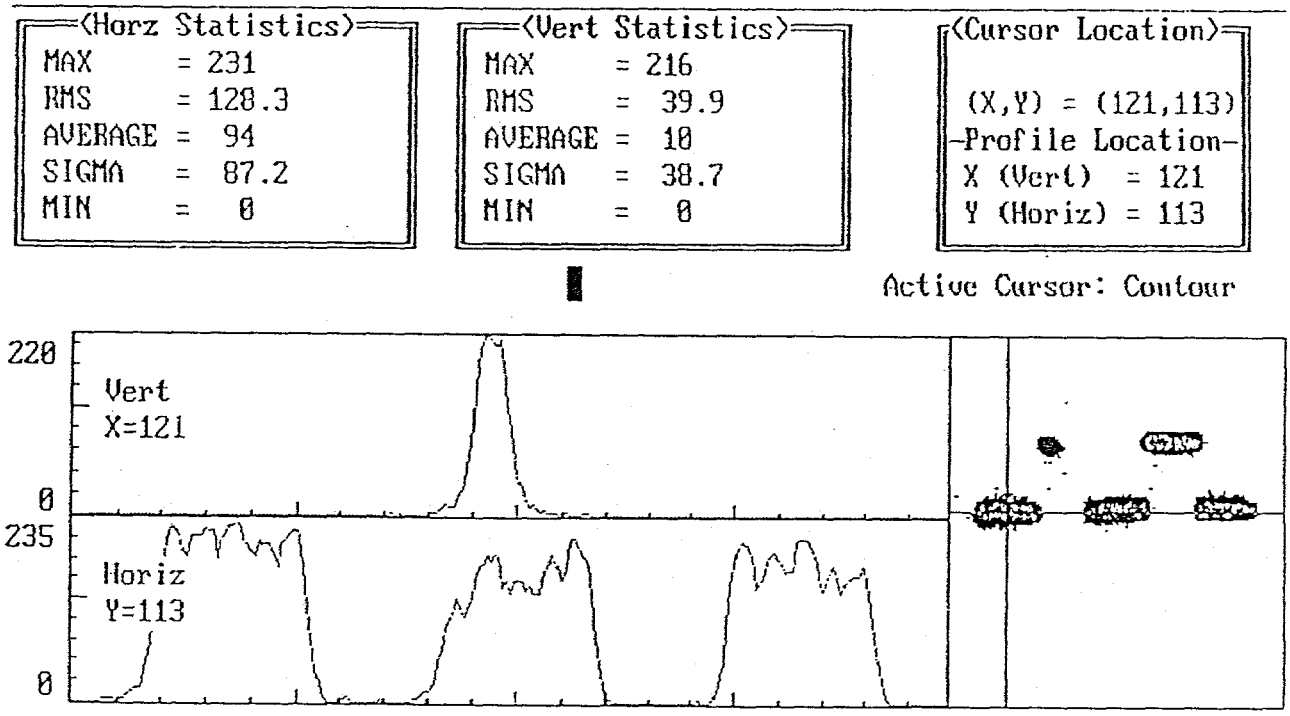

Fig. 13. The PCSS/LDA images obtained from the MCPII/CCD system.

Table 2. The LANL MCPII/CCD response to the SNL PCSS/LDA. The entries show the variety of data obtained for both "warm" and "cooled" conditions of the LDA. Cooled LDA images were about 19 times brighter than those from the warm LDA. The first ratio entry of 58.2 is considered an "outlier" and is cited only for completeness.

File	Images Used	Condition	Mean Intensities Measured with BeamCode					Ratios	
			bar 2	bar 3	bar 4	bar 5	Average		
warm2	(1–10)	warm	3.0	4.0	1.0	3.0	2.8	avg9/avg2	58.2
warm5	(1–60)	warm	10.0	12.0	3.0	7.0	8.0		
warm7	(3,4,5,7,9)	cooled	190.0	109.0	112.0	148.0	139.8	avg7/avg5	17.5
warm9	(1–10)	cooled	156.0	177.0	156.0	166.0	163.8	avg9/avg5	20.5
warm11	(1,4,6,7,8)	warm	4.0	8.0	2.0	6.0	5.0		
warm12	(1,2,3,5,6)	cooled	115.0	101.0	82.0	73.0	92.8	avg12/avg11	18.6

8. REFERENCES

1. I. P. Csorba, *Image Tubes* (Howard W. Sams & Co., Inc., 1985), Section 9.3, "Active Gated Image Intensifier System," pp. 142–143.
2. Matthew C. Thomas, George J. Yates, and Paul Zagarino, "Image Enhancement using a Range Gated MCPII Video System with a 180-ps FWHM Shutter," Proc. of SPIE's 1995 Photoelectronic Detectors, Cameras, and Systems, SPIE Vol. 2551, pp. 174–180, San Diego, California, July 1995.
3. J. L. Detch, Jr. and B. W. Noel, "Radial pulse propagation and impedance characteristics of optically shuttered channel intensifier tubes," Proc. of SPIE's Los Alamos Conference on Optics '81, SPIE Vol. 288, pp. 434–446, Los Alamos, New Mexico, April 1981.
4. N. S. P. King, G. J. Yates, S. A. Jaramillo, J. W. Ogle, and J. L. Detch, Jr., "Nanosecond gating properties of proximity-focused microchannel-plate image intensifiers," Proc. of SPIE's Los Alamos Conference on Optics '81, SPIE Vol. 288, pp. 426–433, Los Alamos, New Mexico, April 1981.
5. G. J. Yates, N. S. P. King, S. A. Jaramillo, J. W. Ogle, B. W. Noel, and N. N. Thayer, "Image shutters: gated proximity-focused microchannel-plate (MCP) wafer tubes versus gated silicon intensified target (SIT) vidicons," Proc. of SPIE's 15th International Congress on High Speed Photography and Photonics, SPIE Vol. 348, pp. 422–433, San Diego, California, August 1982.
6. George J. Yates, Steven A. Jaramillo, Paul Zagarino, Matt Thomas, "Stripline microchannel plate image intensifiers tubes (MCPTS) for nanosecond optical gating applications," Proc. of SPIE's Conference: High Speed Photography, Videography, and Photonics IV, SPIE Vol. 693, pp. 57–62, San Diego, California, August 1986.
7. Matthew C. Thomas, George J. Yates, and Paul Zagarino, "Fast optical gating using planar-lead MCPIIs and linear microstrip impedance transformers," Proc. of SPIE's Conference: Ultrahigh- and High-Speed Photography, Videography, and Photonics '94, SPIE Vol. 2273, pp. 214–225, San Diego, California, July 1994.
8. Fred J. Zutavern, Wesley D. Helgeson, Guillermo M. Loubriel, George J. Yates, Robert A. Gallegos, and Thomas E. McDonald, "A Compact, Short Pulse, Laser for Near-field, Range-gated Imaging, Proc. of SPIE 22nd International Congress on High-Speed Photography and Photonics, Santa Fe, New Mexico, October 1996.